Remote Sensing of Environment 115 (2011) 2292–2301

Contents lists available at ScienceDirect

Remote Sensing of Environment

journal homepage: www.elsevier.com/locate/rse

Modeling moulin distribution on Sermeq Avannarleq glacier using ASTER and WorldView imagery and fuzzy set theory

T. Phillips [a,b,*], S. Leyk [c], H. Rajaram [d], W. Colgan [c,e], W. Abdalati [b,c,e,f], D. McGrath [c,e], K. Steffen [c,e]

[a] Department of Aerospace Engineering and Sciences, University of Colorado, Boulder, CO, 80309, USA
[b] Earth Systems Observation Center, University of Colorado, Boulder, CO, 80309, USA
[c] Department of Geography, University of Colorado, Boulder, CO, 80309, USA
[d] Department of Civil, Environmental and Architectural Engineering, University of Colorado, Boulder, CO, 80309, USA
[e] Cooperative Institute for Research in Environmental Sciences, University of Colorado, Boulder, CO, 80309, USA
[f] Chief Scientist, NASA Headquarters, Washington, DC, USA

ARTICLE INFO

Article history:
Received 27 December 2010
Received in revised form 15 April 2011
Accepted 16 April 2011
Available online 31 May 2011

Keywords:
Cryosphere
Fuzzy set theory
Surface melt
ASTER DEM
Ablation zone

ABSTRACT

A fuzzy set overlay model is used to analyze the distribution of moulins (vertical meltwater conduits) on Sermeq Avannarleq ("Dead Glacier") in West Greenland in 1985 and 2008–09. Input data is derived from a historical topographic map based on airborne visible imagery and more recent WorldView-1 panchromatic imagery, as well as an Advanced Spaceborne Thermal Emission and Reflection Radiometer (ASTER) digital elevation model (DEM). A non-parametric best-fit model approach using a Monte Carlo simulation is used to derive the membership functions for moulin location based on three independent variables – elevation, slope and aspect – and to test for the robustness of the model. We determine that there is a topographic setting independent of time that favors the development of moulins in this region. Using the membership functions, and an optimal alpha cut derived for 1985, we could correctly predict the locations of ~88% of the moulins in 2008–09. The model accounts for increased surface melt in 2008–09 in comparison to 1985. Our results demonstrate the potential of a fuzzy set based approach to improve models of ice sheet hydrology in Western Greenland, by providing more reliable spatial distributions of entry points of meltwater into the ice based on remotely sensed datasets of the ice surface, which are readily available.

1. Introduction

The Greenland and West Antarctic Ice Sheets are currently losing more mass through meltwater runoff and iceberg calving than they are gaining through snowfall, indicating they have a negative mass balance (Alley et al., 2005; Rignot et al., 2008a,b; Velicogna & Wahr, 2006). Observations on the Greenland Ice Sheet (GrIS) suggest that it is losing mass at a rate that has doubled over the last decade to 267 ± 34Gt/year for the period 2000–2007 (Rignot et al., 2008a). It is believed that approximately 60% of the mass loss of the GrIS for the period 2000–2008 occurred through iceberg calving, dominated by a few outlet glaciers, while the remaining 40% is due to surface melt runoff (Van den Broeke et al., 2009). Widespread acceleration has been observed on outlet glaciers such as the Jakobshavn Glacier, which doubled its velocity in the last 10 years. Glaciers and ice sheets were long thought to respond slowly to climatic perturbations (Hooke, 2005; Paterson & Cuffey, 2010); and the mechanisms by which a warming climate could accelerate glacier flow on as short a time scale as a decade, are not yet fully understood. Recent acceleration of the Jakobshavn Glacier has been attributed to various mechanisms such as meltwater-induced basal lubrication and changes to the terminus geometry lead to a reduction in back-stress (Howat et al., 2008; Joughin et al., 2008; Rignot & Kanagaratnam, 2006; Zwally et al., 2002). The basal lubrication mechanism requires water to penetrate the ice and reach the bed through the englacial hydrologic system (Catania & Neumann, 2010; Zwally et al., 2002). Due to the fractured nature of the ice sheet, a large fraction of surface meltwater generated at the surface enters the ice sheet through crevasses and moulins (Fig. 1) and eventually reaches the glacier bed (Catania & Neumann, 2010). Strong correlations between the timing and rate of surface meltwater production and changes in ice velocity on the GrIS (Colgan et al., 2011) substantiate this mechanism. Phillips et al. (2010) suggested that meltwater flow through the englacial hydrologic system can warm the ice, thus potentially affecting ice rheology and ultimately flow velocity (Fountain et al., 2005). Quantification of these mechanisms is important for predicting ice sheet response to climate warming, and requires an improved understanding of the water discharge through the englacial hydrologic system, which is in turn controlled by the spatial density of water entry points (i.e. crevasses and moulins).

Moulins, nearly vertical conduits in the ice formed and maintained by flowing water, are seasonally active features of the cryo-hydrologic

* Corresponding author at: Department of Aerospace Engineering and Sciences, University of Colorado, Boulder, CO, 80309, USA. Tel.: +1 303 492 4829.
E-mail address: Thomas.Phillips@colorado.edu (T. Phillips).

0034-4257/$ – see front matter © 2011 Elsevier Inc. All rights reserved.
doi:10.1016/j.rse.2011.04.029

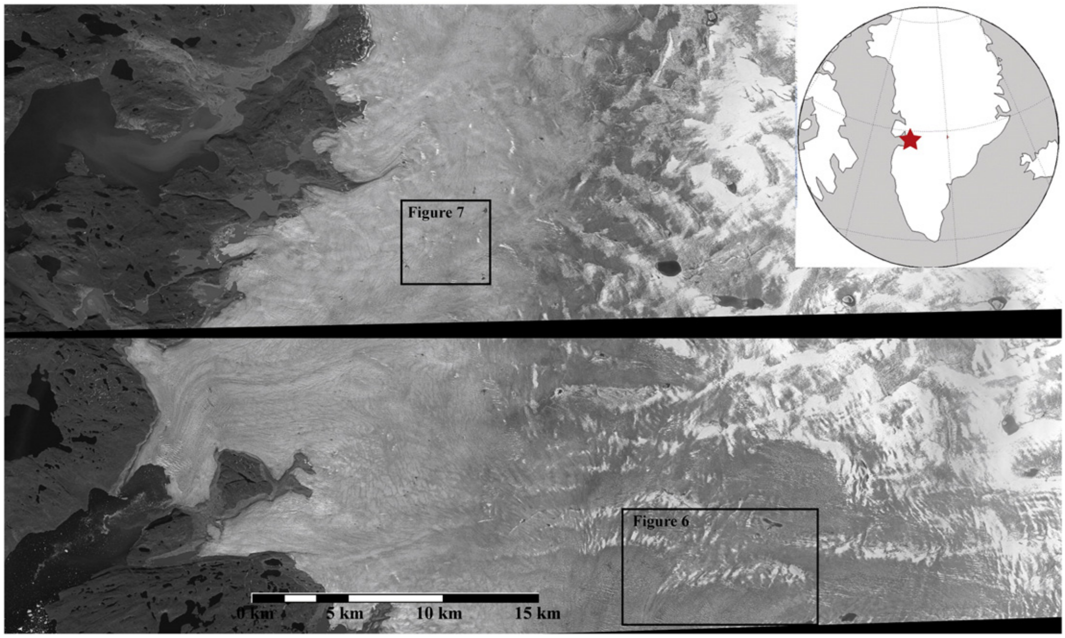

Fig. 1. The Sermeq Avannarleq Glacier is located in Western Greenland (star). The two frames indicate the geographical locations of Figs. 6 and 7. The background is the 2009 Worldview Image used for locating moulins.

system. They are usually found downstream of a crevasse field in a relatively flat section of a glacier. Crevasse fields, which typically occur in regions of high extensional strain near the surface precondition the ice for moulin formation (Hooke, 2005). Even though crevasses may close due to compression as they are advected downstream, the thermal energy of meltwater and viscous heat generation allows moulins to remain open (Holmlund, 1988). In order to predict moulin locations from first principles using a physically based model, ice stress and strain rates need to be calculated. This requires good knowledge of ice velocity and basal topography, which are often not readily available (Hooke, 2005). On smaller glaciers, moulins are sometimes advected out of their catchments within a single year, resulting in a "string of pearls" of abandoned moulins, with new active moulins forming upstream (Holmlund, 1988; Reynaud, 1987). In Western Greenland, Catania and Neumann (2010) estimate average moulin lifetimes of the order of 11 years, ranging even up to 44 years. There is some evidence suggesting that the englacial network survives throughout the winter, allowing meltwater to use the same englacial channels and conduits for multiple years (Gulley & Benn, 2007).

The climate along Greenland's west coast has experienced above average warming in the late 20th century. This has resulted in a rise of the equilibrium line altitude by up to 350 m, increasing both the area over which surface melt occurs and the total volume of meltwater production (Fausto et al., 2009; Hanna et al., 2008; van den Broeke et al., 2009). In a relatively large area of Western Greenland (60 N to 70 N), there is a systematic zonation of supraglacial hydrologic features, with large lakes forming in the "dark zone" above 900 m elevation in the 1990s, where ice exhibits less fracturing, slopes are flat (<2°) and runoff generation rates are low (Greuell, 2000). The large ice thicknesses in this region could also prevent hydrofracture propagation to the bed, which promotes moulin formation beneath supraglacial lakes. Downstream of the "dark zone", runoff generation rates are higher, and crevasses/moulins form in an elevation band that ranges from 300 m to 800 m, with a width ranging from 70 to 150 km. In this elevation band (hereinafter referred to as the "runoff zone"), moulins typically do not occur in regions with significant crevassing. At lower elevations, intense crevassing prevents the formation of moulins by intercepting runoff. In this paper we focus on using an approach based on remote sensing and surface observations to understand the distribution and location of moulins within the runoff zone. Moulins created due to episodic massive lake drainage events (Das et al., 2008) in the dark zone are less common and not considered in this study. Our approach does not incorporate information on physical processes controlling crevasse formation, which is necessary for moulins to form. In order to do so, a process-based model for calculating stresses and strain rates would be required, which would in turn require high-resolution bed topography data, which is seldom readily available. On the other hand, high-resolution satellite imagery and DEMs are becoming increasingly available, providing the first-order ice geometry datasets used in this study. As noted above, there is an extensive zone of the order of 10^5 0km^2 in Western Greenland where moulins are observed to occur.

This paper investigates the distribution of moulins in the runoff zone of the Sermeq Avannarleq (just north of Jakobshavn Glacier) in Western Greenland, in 1985 and 2008–09, using a fuzzy overlay model driven by first-order local ice topography features (at ~100 m scale). Our fuzzy overlay model is based on best-fit fuzzy membership functions that are assigned using a non-parametric statistical approach and Monte Carlo simulations, to compute membership degrees for moulin occurrence as a function of the customary first-order topographic variables: elevation, slope and aspect (the direction of slope with respect to north = 0). The reasons for our choice of independent variables are as follows: (i) as noted above, moulins in Western Greenland largely occur within an elevation band that we have referred to as the runoff zone above; elevation is also a proxy for surface meltwater generation; (ii) several studies (Holmlund, 1988; Reynaud, 1987) suggest that moulins typically occur in regions with low local slope downstream of crevasses, and (iii) aspect serves as a proxy for incoming shortwave radiation by determining the extent to which the slope is north-facing.

Our approach incorporates tests for the robustness of relations between moulin presence and topographical characteristics that are believed to be important factors for a moulin to form (Piccini et al., 2002; Reynaud, 1987). Fuzzy overlay analysis is carried out to determine locations of highest likelihood for moulin occurrence by combining the explanatory topographic factors using different fuzzy logic operators in a spatial model framework. We derived the fuzzy membership functions based on moulin locations and topographic features for 1985. Subsequently, we apply these membership functions to determine moulin locations in the increased area experiencing melt in 2008–09. We compare the predicted moulin locations for 2008–09 to WorldView imagery detections as well as the surface drainage system derived from the 2008 ASTER DEM to demonstrate the robustness of our approach. The fuzzy logic model exhibits great potential for use in estimating evolving moulin density in the ablation zone of the Greenland Ice Sheet, an important first step in constraining hydrologic inputs that can influence accelerated flow and cryo-hydrologic warming.

2. Fuzzy sets and imprecise phenomena

Fuzzy logic is a form of multi-valued logic that deals with reasoning, which is approximate rather than precise and is based on fuzzy set theory (Zadeh, 1965). Fuzzy set theory is appropriate where there is inherent vagueness in the boundary conditions between classes (i.e. the wet to dry snow classification spectrum; Key et al., 1989) or in the definition of a class if the phenomenon or process of interest is ill defined (i.e. moulin development). Fuzzy set theory, in combination with geospatial analysis, has been applied to a wide range of problems including soil mapping (Burrough, 1989; McBratney & Odeh, 1997), terrain modeling (Deng & Wilson, 2008; Fisher et al., 2004), cartographic generalization (Anderson-Tarver et al., 2011), land cover change (Leyk & Zimmermann, 2007), land use analysis (Fritz & See, 2005), landscape ecology (Bolliger & Mladenoff, 2005) and basal glacier hydrology (Corne et al., 1999). There has been no previous quantitative study on the spatial distribution of moulins on an ice sheet. Due to the inherent uncertainty in characterizing/predicting moulin locations, fuzzy set theory represents an appropriate approach for this problem.

Unlike in classical set theory where according to the Boolean approach an object is either a member of a class or not, fuzzy sets account for partial membership and/or multiple memberships to different classes (Zadeh, 1965). For example, using fuzzy set theory, the same location can be classified as wet snow to a certain degree as well as ice to a certain degree, whereas a Boolean classification would classify it as either snow or ice despite both appearing within the pixel in question. The phenomenon of multi-memberships in this instance results from non-crisp transitions between the classes of water, wet snow and ice. A pixel in an image is not necessarily covered only by ice but can also include some area proportion covered by snow (Key et al., 1989). Fuzzy set theory allows each element of interest to be assigned degrees of membership in a fuzzy set on a gradual scale in the real unit interval [0, 1] using fuzzy membership functions. The definition of membership functions can be based on standard function types (Robinson, 2003) or determined from data using the Semantic Import (SI) model (Robinson, 1988). Fuzzy sets generalize classical (Boolean) sets, since the indicator functions of classical sets are special cases of the membership functions of fuzzy sets, if the latter only take values 0 or 1 (Dubois & Prade, 1988). For this reason classical Boolean sets are referred to as “crisp” sets.

In our present study, fuzzy logic is used to predict potential moulin locations. Similar to other objects with non-distinct boundaries, such as clouds, moulins can only be understood in the context of underlying conditions — in this case for terrain and water availability. While there is some agreement on what defines a moulin (Holmlund, 1988; Piccini et al., 2002; Reynaud, 1987) the distribution of moulins and the topographic factors that influence moulin development have not been mathematically quantified. This lack of knowledge of the influences of terrain and meteorological variables on moulin development, as well as the interactions of these independent variables, inhibits the prediction of moulin development locations using classical set theory. Thus, the likelihood of moulin development at a location represents an imprecisely defined phenomenon, for which a fuzzy logic model is ideally suited.

3. Field site and data

The study site for this investigation is the ablation region of the Sermeq Avannarleq (“Dead Glacier”) drainage basin in West Greenland, located just north of Jakobshavn Glacier. The runoff zone in this region shows steeper overall surface slopes than the dark zone (>4° versus <2° respectively) (Greuell, 2000). Within the runoff zone, moulins typically form in locations that exhibit relatively low surface slopes that allow the concentration of runoff (Holmlund, 1988). The drainage basin is approximately located at 69°25′ N and 49°55′ W (Fig. 1). The glacier snout is at 69°22′ N and 50°25′ W, where it calves icebergs into a side arm of the Jakobshavn Fjord. The study area is an approximate rectangle of 750 km^2 (30 km × 25 km). The Sermeq Avannarleq has experienced a negative mass balance beginning in 1985, with a maximum retreat of the terminus of 2 km over the last 26 years (Colgan et al., 2011).

The Greenland Geological Survey (GEUS; Thomsen, 1986; Thomsen et al., 1988) has compiled a 1:75,000 supraglacial hydrology map of the Sermeq Avannarleq ablation zone based on panchromatic aerial photography obtained on 10 July 1985. This map delineates features such as crevasse fields, surface lakes and rivers as well as moulins. A total of 318 moulins were identified within the map extent. Unfortunately, neither the map nor the supporting documentation (Thomsen, 1986) indicates the criteria or methodology used to identify the moulins. Our own field observations, conducted in August 2008 and 2009, and supplemented with an ~55 cm panchromatic WorldView-1 image acquired on 15 July 2009, suggest that the GEUS map likely only identifies moulins with a diameter > 1 m. From field observations we estimate that up to 5 times as many unidentified moulins of much smaller diameter (i.e. <1 m) exist within the map area, possibly clustered around the larger moulins identified in the GEUS map. The GEUS supraglacial hydrology map was scanned and georectified in a Geographical Information System (GIS). Moulin locations (318 in 1985) and ice elevation contour lines (equidistance of 10 m; from 0 to 1180 m elevation; point spacing of ~250 m) were manually digitized. The digitized elevation points (total of 9306) were interpolated using a minimum curvature spline technique to create a digital ice elevation model (DEM) with a horizontal resolution of 125 m for the year 1985. The stated absolute vertical accuracy of the GEUS map is ±30 m (Thomsen, 1986).

The moulin distribution across the study site was also examined for 2008 using the latest available ASTER DEM (derived primarily from 2008 imagery). The ASTER global DEM has a horizontal resolution of 30 m with absolute vertical and horizontal accuracies of ±20 m and ±30 m, respectively. Three topographic variables – elevation, slope and aspect – were extracted from the DEM with a resolution of 125 m. These variables were chosen as a first-order set of independent explanatory variables for describing the potential for a moulin to form at a given location, which represents the dependent variable in the study.

4. Methods

Fuzzy logic, which has been conceptualized for vague geographies by Fisher (2000), has recently been applied to combine spatial variables (i.e., fuzzy overlay) to produce coherent final maps (Arnot et al., 2004; Fritz & See, 2005). Zadeh (1965) proposed three basic operators: (i) complement, (ii) union and (iii) intersection, which have been extended and combined by various authors (Klir & Yuan, 1995; Yager, 1980). Robinson (2003) summarized fuzzy logic operators that have been proven useful in analyzing spatial and temporal variabilities using GIS and remote sensing technology.

We assign fuzzy membership functions for the independent variables (elevation, slope and aspect) based on iteratively simulated subsets of the underlying data in order to assign the membership degree of each pixel to the prototype concept of a perfect moulin location. The resulting fuzzy surfaces are then input to a fuzzy overlay procedure using fuzzy logic operators to model the likelihood for moulin occurrence based on the described independent variables and their interactions.

In order to statistically determine and justify the assignment of robust membership functions for each independent variable, the distributions in co-location with field-observed moulins in 1985 were systematically examined and the three variables were tested for independence so that no variable is over-weighted and no bias is generated. The approach presented here consists of four steps: testing the moulin distribution and the variables for independence (Section 4.1), deriving the membership function for each variable (Section 4.2), carrying out fuzzy overlay to produce a fuzzy membership map (Section 4.3), and using appropriate alpha cuts (e.g. threshold values defining a location as containing a moulin or not) to produce a 1985 categorical moulin likelihood map (Section 4.4). A second moulin likelihood map was then produced for 2008 (Section 4.5).

4.1. Testing total and moulin-co-located distributions and independence of variables

The histogram for the distribution of the moulin-co-located subset of each independent variable was compared with the overall distribution of that independent variable for the Sermeq Avannarleq basin using the Wilcoxon-Rank Sum test to ensure that the distribution of underlying moulin locations is different from the total distribution (Montgomery & Runger, 2006).

Rather than using the absolute distribution of occurrences we calculated the frequency per bin of occurrences, which is the number of moulins observed for a specified range of values of variable x (i.e., which belong in a particular bin) divided by the total number of observations of values x in that bin. For example if moulins occurred on 4 pixels of a given bin, and a total of 10 pixels across the study site are in that bin, the frequency per bin would be 0.4. We tested for correlation between independent variables in order to assure that they were truly independent, to avoid model bias due to co-linearity (Montgomery & Runger, 2006).

4.2. Deriving non-parametric best-fit membership functions

We derived best-fit functions for the histograms of the moulin co-located subsets of the independent variables using Monte Carlo simulations to robustly approximate the underlying distribution. This process was repeated 500 times using subsets of 150 moulins randomly picked for each of the iterations. To do so we used non-parametric models since the frequencies of all independent variables followed non-Gaussian distributions with multiple peaks. The use of Monte Carlo simulation allowed us to test if different moulin-co-located subsets of independent variables produce similar membership functions and thus, to statistically examine the robustness of membership assignment. In Fig. 2 the distribution of the elevation (Fig. 2a), aspect (Fig. 2b) and slope (Fig. 2c) is shown as box plots showing the variation and hence robustness of each variable. The outliers are shown as circles. The resulting membership functions quantify the relationship between moulin occurrence (i.e., the possibility for a moulin to occur at a location) and the independent variables as derived from the observed moulin-co-located distribution. Fig. 2 clarifies the validity of the chosen independent variables in controlling moulin occurrence. The likelihood of moulin occurrence is highest for elevations in the range of 300–800 m, which corresponds to the runoff zone. Aspect values around 55° are most favorable for moulin occurrence. Closer examination revealed that the river channels feeding most moulins are on south and southwest facing slopes. Moulins form at topographic depressions at the bottom of such slopes, extending slightly into the opposite slope, where the moulin location is maintained at a lower elevation by downcutting at very small scales. Moulin locations are also largely concentrated in very low slopes (Fig. 2c).

We normalized the membership functions by stretching the mean of the maximum frequency to unity and setting the minimum frequency to zero (Fig. 2d–f). This step was done in order to describe how favorable each location is for a moulin to develop. A location with a membership function value of zero has no similarity with the perfect conditions for a moulin to form. A location with a membership function value of 1, however, is the perfect location for a moulin. The normalized membership functions were included in the fuzzy overlay model described in Section 4.3.

4.3. Spatial fuzzy overlay model

We carried out fuzzy overlay using fuzzy logic operators to model for each pixel the possibility for a moulin to develop based on the three independent variables and their interactions. Fuzzy operators can be formalized as “intersection” (AND), which corresponds to the limiting MIN operator, or “union” (OR), which is interpreted as the MAX operator. Different versions of these fuzzy operators have been described (Yager, 1995) and successfully applied in a GIS framework (Robinson, 2003) and in remote sensing (Key et al., 1989).

Logical operators can be combined and adapted to model different types of complex interactions between variables. For example, intersection can be used to implement a limiting variable by assigning the minimum membership value (logical AND operation) to the overlay of this variable with one or more other variables. Alternatively, the union operator can be used to combine variables that could compensate each other (i.e., appear to have independent impact on moulin development and hence only one of the two variables is necessary for the moulin development) by assigning the maximum value (OR operation). The result of fuzzy overlay operations is a new fuzzy set represented as a spatial fuzzy surface.

We used the connective union operator (Yager, 1980) to overlay the fuzzy surfaces of aspect (a) and slope (s) since these two factors can be conceptualized as compensating variables that represent proxies for ice flow direction and velocity. Hence, the variables a and s are assumed to be independent drivers for moulin development (Fountain & Walder, 1998; Piccini et al., 2002; Reynaud, 1987). In Eq. (1) below, we denote the fuzzy membership function for aspect (a) by $A(a)$, and that for slope (s) as $S(s)$. The connective union operator is of the form:

$$A \vee S = min\left\{ \left[A^p + S^p\right]^{1/p}, 1 \right\}. \quad (1)$$

Where p is the power number to be used to unify slope and aspect. We used $p = 0.5$ as suggested in Robinson (2003). $\vee$ is the logical union operator.

We used the connective intersection operator (Yager, 1980) to overlay the result of the union of slope and aspect ($(A \vee S)$ in Eq. (2) with the fuzzy set of elevation (E in Eq. 2 below), under the assumption that elevation is a proxy for the mean annual temperature of the Greenland Ice Sheet and hence for the amount of surface meltwater generated (Cuffey & Clow, 1997). As noted above, at higher elevations (i.e. in the dark zone), meltwater generation is insufficient for moulins to form. Additionally, the ice thickness is also potentially too large for hydrofracturing to occur. Although sufficient meltwater is generated at the margin (lowest elevation), heavy crevassing prevents the formation of moulins. Thus, there is an intermediate range of elevation (previously defined as the runoff zone) where moulins are most likely to occur. Consequently elevation is implemented as a limiting variable. The connective intersection operator allows tuning of the power function

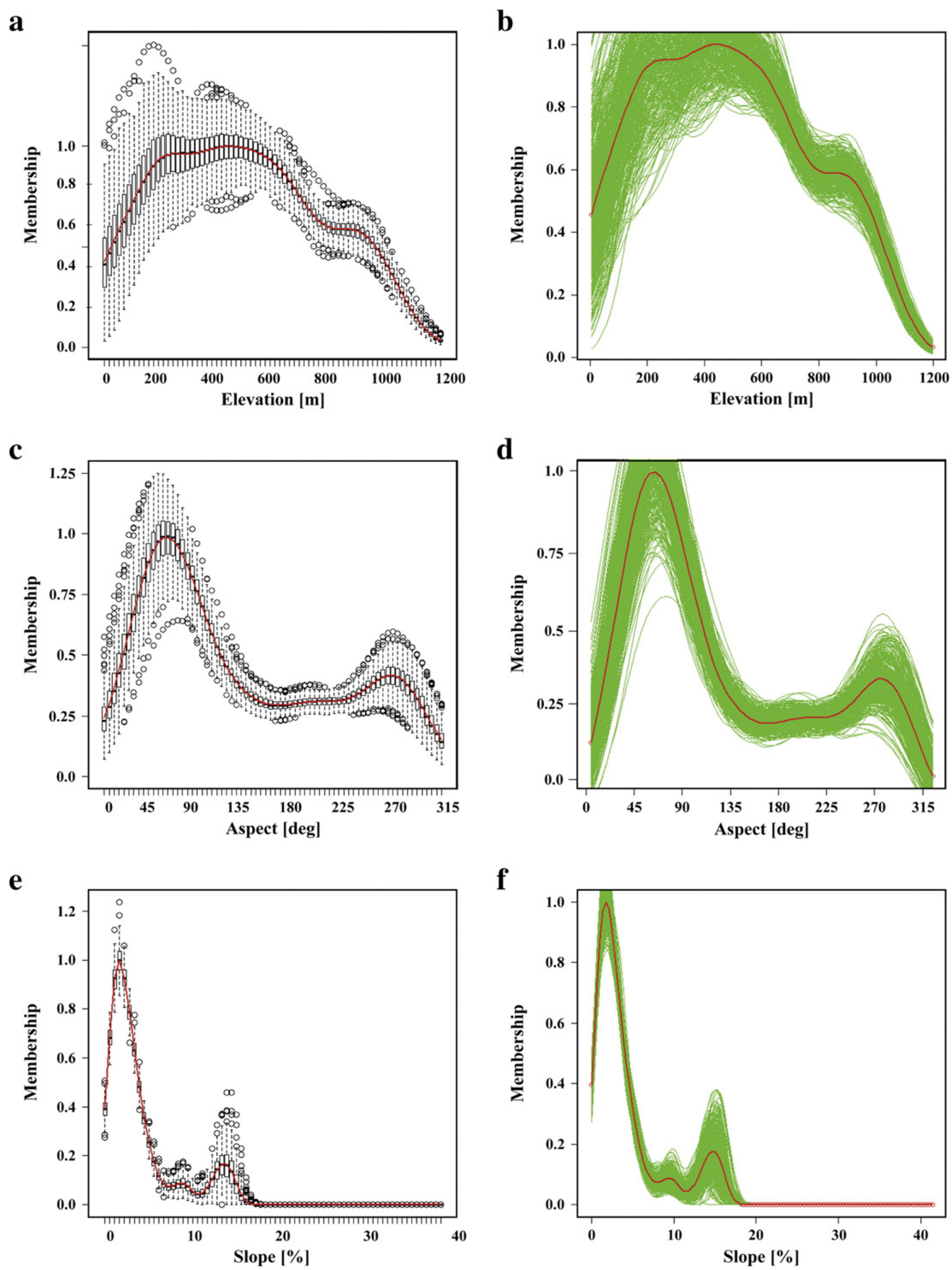

Fig. 2. (Left): Box plots for the number of moulins/km^2 as a function of elevation (a), aspect (c) and slope (e). (Right) Individual membership functions for all 500 Monte Carlo simulations (green) and their average (red), which was used as the membership function. The average membership functions were normalized in such a way that the minimum value was set to zero and the mean of the maximum was set to 1.

and hence the integration of non-linear dependency of the relationship, with the form:

$$C(a,s,e) = (A\vee S)\wedge E = 1 - \min\left\{\left[(1-(A\vee S))^{p} + (1-E)^{p}\right]^{1/p}, 1\right\}. \quad (2)$$

In Eq. (2) $(A\vee S)$ is the fuzzy union of slope and aspect (see Eq. 1) that is intersected with the fuzzy set of elevation E and p is the power number in order to describe non-linear relationships. The result is a tri-variate membership function $C(a, s, e)$ that ranges from 0 to 1, and may be used to evaluate the likelihood of moulin occurrence at a given location.

4.4. Mapping moulin occurrence likelihood in 1985

The fuzzy surfaces are used to create likelihood maps, indicating for each pixel the level of likelihood for moulin development. In order to define crisp categories of likelihood we carry out a defuzzification mainly to accommodate better interpretation of the results for users who are used to explore risk zones as crisp entities. This process is based on a cutoff value, which is referred to as the alpha cut.

The fuzzy surface of $(A \vee S) \wedge E$, i.e. the tri-variate function $C(a, s, e)$, is the result of overlaying aspect a, slope s and elevation e at each grid cell. If $C(a, s, e) > \alpha$ (alpha cut *value* $0 \leq \alpha \leq 1$) it is assumed that a moulin occurs. Hence each pixel, which is assigned a membership degree equal to or greater than the alpha cut is included in the considered likelihood category. The assignment of the alpha cut value represents an important decision in the cartographic presentation of the results and can potentially affect the outcome of the analysis (Robinson, 2003).

A low alpha cut will include a large percentage of field-observed moulins correctly classified as moulin likelihood areas. A low alpha cut value, however, also overestimates the area in which moulins are likely to form. Conversely, a high alpha cut value will result in a lower number of moulins correctly being identified, as well as a smaller total area of high moulin likelihood. In order to identify the areas of transition between low and medium and medium and high likelihood we tried to find the range of alpha cuts in which the percentage of moulins being classified correctly decreases rapidly. Areas of membership degrees greater than the upper boundary of the transitional class are considered “high likelihood” areas, whereas values less than the lower boundary are classified as “low likelihood” areas.

The lower boundary and upper boundary are selected by means of comparing the change in the number of correctly classified moulins as a function of the alpha cut value. When plotted in a cumulative curve plot, where 0 represents no moulin and 1 describes definite moulin occurrence, 100% of the field-observed moulins and all pixels in the study area are expected to be included if the alpha cut is set to zero. Conversely most moulin locations and pixels in the study area would be classified as no likelihood areas if the alpha cut was close to 1. If the cumulative curve transitions from 0 to 100% membership within a small range of alpha cut values, the system is considered to be crisp and selecting an appropriate alpha cut is an easy task. In the case of a smooth transition over a broad range of fuzzy membership values, the selection of an alpha cut is more difficult and is an issue frequently encountered in constructing fuzzy classification schemes for natural phenomena (Arnot et al., 2004). In general the medium likelihood level represents a class of possible transition (high variation in membership values) to low or high likelihood in which the class-specific area can change drastically for even small changes in the alpha cut.

4.5. Mapping moulin locations for 2008–09

In order to create a moulin likelihood map for the years 2008–09, we used membership functions derived for 1985 and applied them to the resampled ASTER 2008–09 DEM at the same resolution of 125 m. First, the moulin locations extracted from the ASTER DEM were validated based on two sub-regions (identified with boxes in Fig. 1) from the WorldView-1 Imagery for 2009 and field observations from 2006 to 2008 (which confirmed that moulin locations remain at more or less the same location for a few years). These two subregions cover only 7–8% of the overall region of interest. Due to the lack of adequate imagery, the above approach could not be applied over the entire study area. Outside of the two sub-regions mentioned above, we derived the moulin locations for 2008–09 using the surface runoff accumulation model offered in ESRI ArcGIS (Tarboton et al., 1991), which calculates the catchment size for each pixel based on elevation and flow direction (steepest slope).

We first attempted to correlate moulin locations in 1985 with surface runoff accumulation. Using the estimated surface mass balance for the Sermeq Avannarleq and the catchment areas for each moulin in the late 1980s (Thomsen et al., 1988), we were able to calculate the approximate total volume of water available at each moulin location in 1985. We found that moulins were statistically almost never observed in pixels that drain a runoff volume lower than 450,000 m^3/year. We thus used this value as a threshold to prescribe moulin locations for 2008–09. Establishment of a hydrologic connection to the glacier bed through a crevasse by hydrofracturing is typically determined by the background tensile stress, ice thickness and availability of surface meltwater (van der Veen, 2007). Between 1985 and 2007, all these factors are likely to have changed significantly. However, van der Veen (2007) also shows that the water-filling rate is the most important factor controlling crevasse propagation. For this reason, and also because we are exploring an approach based on readily available topographic information, we believe that our use of the threshold runoff volume of 450,000 m^3/year for 2008–09 is reasonable. The Sermeq Avannarleq surface ablation (meltwater production) rates presented in Fausto et al. (2009) were used to calculate the melt volume generated at each pixel in 2008–09. Surface runoff accumulation was then calculated over the entire study area, including higher elevations that did not experience melt in 1985. Moulins were assumed to occur in pixels where the surface runoff accumulation exceeded 450,000 m^3/year, and a proxy dataset of potential moulin locations in 2008–09 was thus created. The moulin surface likelihood predicted by the membership functions was then compared to the above proxy dataset in order to account for the regions, which had experienced melt for the first time between 1985 and 2008–09 and thus relaxing the elevation constraint.

5. Results

We analyzed the percentage of all moulins correctly estimated in moulin likelihood zones for each alpha cut between 0.2 and 0.9 at intervals of 0.1 (Fig. 3). As suggested in Section 4.4, the total area considered as at moulin likelihood decreases with increasing alpha cut value for 1985. According to Fig. 3a the entire ablation zone is at moulin likelihood for an alpha cut of 0.2. This does not reflect the reality that moulins are sparse features, as a lack of surface meltwater or limited catchment area makes certain locations unsuitable for moulin formation. For high alpha cut values (e.g., 0.8 and 0.9) (Fig. 3g and h) the area of the likelihood zone decreases to a very small area, which is also not realistic as moulins are found throughout the ablation zone. This quantitative comparison (Fig. 3a–g) illustrates the need for an in-depth analysis of the distribution of moulins as a function of the alpha cut level.

Fig. 4 shows the distribution of pixels and moulin-containing pixels with different membership values of $C(a, s, e)$ for the ablation zone of the Sermeq Avannarleq in 1985. Most of the pixels correspond to low $C(a, s, e)$ values between 0 and <0.4. However, none of these pixels contain moulins. The number of pixels with high membership values is very small. The mean value of the membership function for the entire ablation zone is 0.31. The number of pixels containing moulins is a small fraction of the total number of pixels. Moulins are found in pixels with $C(a, s, e) > 0.4$, and the highest number of moulin-containing pixels correspond to $C(a, s, e) \geq 0.7$. For this reason a more detailed version of Fig. 4a for $C(a, s, e) \geq 0.65$ is shown in Fig. 4b. The mean $C(a, s, e)$ value for the extracted moulin locations in 1985 is 0.66. Fig. 4c shows the fraction of pixels in each $C(a, s, e)$ class that contain at least one moulin. The use of $C(a, s, e)$ as a membership function for identifying moulin locations is justified by the fact that almost all pixels with $C(a, s, e) \geq 0.95$ contain moulins. However, because the number of pixels with such high values of $C(a, s, e)$ is rather small compared to the overall number of pixels, it is also clear that using an alpha cut value of 0.95 would severely underestimate moulin locations. Fig. 4c suggests that it is reasonable to divide the range of membership values into three sections by using two break points that

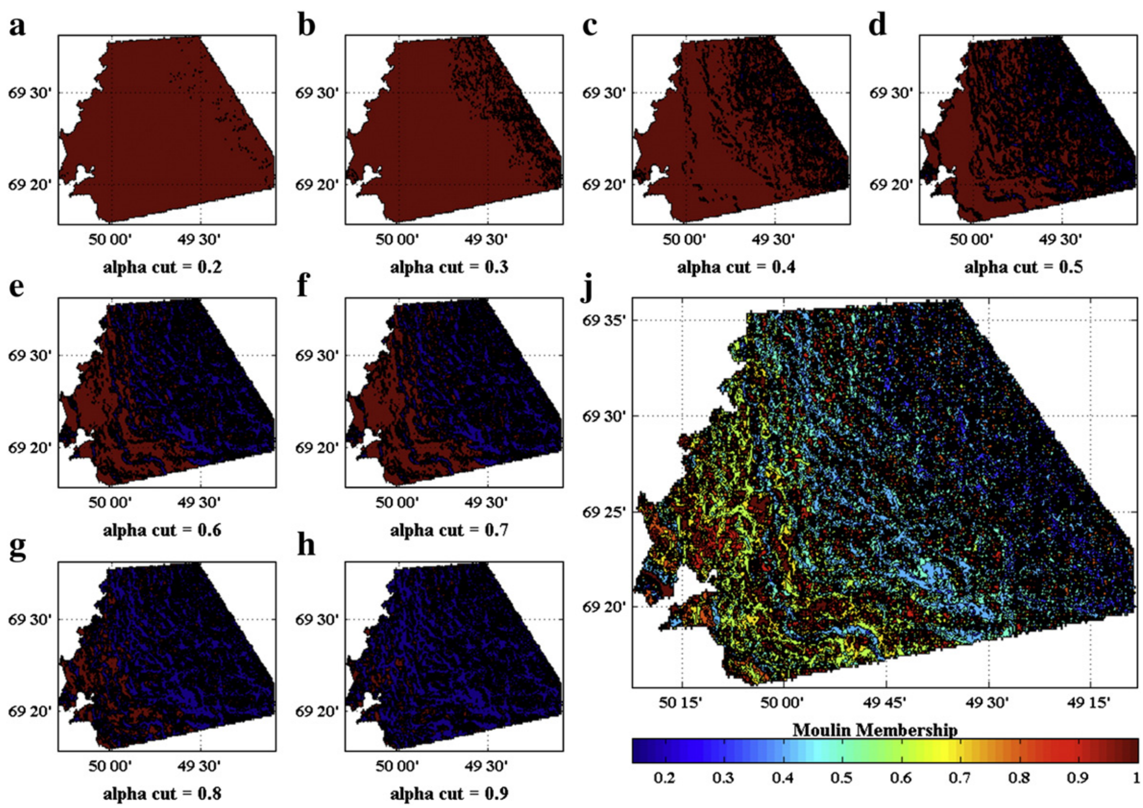

Fig. 3. Defuzzification result to classify moulin likelihood (red) and non-likelihood (blue) across the study area for alpha cuts ranging from 0.2 to 0.9 is shown in figures a)–h). Figure j) shows the fuzzy membership map for the ablation zone of the Sermeq Avannarleq glacier for 2008. The likelihood/non-likelihood maps are based on this fuzzy membership map.

differentiate low ($C(a, s, e) < 0.4$), medium ($0.4 \leq C(a, s, e) \leq 0.8$) and high ($C(a, s, e) > 0.8$) likelihood classes. Locations in the ablation zone with $C(a, s, e) < 0.4$ have a probability of less than 3% of containing a moulin, while locations with $C(a, s, e)$ values between 0.4 and 0.8 have a probability of between 15% and 32% of containing a moulin, and locations with a value of $C(a, s, e) \geq 0.8$ have a probability of between 57% and 96% of containing a moulin.

We defined the likelihood classes in 2008–09 based on the same alpha cuts that were derived for 1985 (0.4 for low likelihood and 0.8 for high likelihood). As a result, 90% of the moulins of the year 2008–09 were located within the medium or high likelihood areas; 41% were located within the high-likelihood area (Fig. 5). There is little variability in the percentage of moulins correctly classified for alpha cuts less than 0.4 and greater than 0.8 (Fig. 4c), which provides evidence that the break points 0.4 (90%) and 0.8 (41%) are robust.

In the two sub-regions in Figs. 6 and 7, where actual moulin location data are available, the fuzzy membership function predicts 634 moulins, while the observations indicated 441. Of the 441 observed moulin locations, the membership function correctly predicted 88.2%. As noted in Section 4.5, moulin locations over the entire region of interest were prescribed using a surface runoff accumulation model to create a proxy dataset. The moulin locations predicted by the membership function were compared to the proxy data. We predicted a total number of 3124 moulins for 2008–09 (Fig. 5). This is approximately ten times the number of moulins observed in 1985. The membership function also predicted moulins at higher elevations for 2008–09 than for 1985 (maximum elevation X versus Y respectively). This is likely due to an upward migration of the equilibrium line altitude and an accompanying expansion of the area where surface meltwater is generated (Fausto et al., 2009). In addition, an increased number of moulins were predicted in lower regions of the ice sheet in 2008–09 as compared to 1985. These moulins were probably not recognized in 1985 because of their smaller dimensions, or they could have formed since 1985 because of increased surface melt. Despite an increase in crevassed area within the Sermeq Avannarleq ablation zone between 1985 and 2009 of 13 ± 4% (Colgan et al., 2011), the number of supraglacial river networks seemed to have increased. The areal extent of each individual catchment has decreased, however the amount of meltwater generated in each catchment has increased, such that there is enough water available to sustain more moulins. The membership function correctly predicted more than 90% of the moulin locations indicated by both real data (in the two sub-regions) and proxy data (full region).

A closer inspection of predicted and verified moulins in 2008–09 in sub-regions where WorldView-I imagery is available shows that the moulins seem to form at the edge of patches of medium and high-likelihood areas (Fig. 6). If the ice flow direction is taken into account one can see that most of the verified moulins are located at the upstream edge of the high-likelihood areas. We calculated an average of 12 moulins/km^2, with a maximum value of 27/km^2 for 2008–09. The density of moulins, however, varies greatly: there are fewer moulins at high elevation (i.e. the accumulation zone) and in steep terrain (i.e. near the ice margin due to the presence of crevasses and poorly defined drainage basins).

Fig. 7 shows a subregion of the Sermeq Avannarleq ablation zone, with the moulin likelihood categories overlain by the 2008–09 ASTER derived water accumulation flow channels (in blue). The dark red areas represent high likelihood for moulin development (alpha cut = 0.8), the orange areas medium likelihood (alpha cut = 0.4) and the remaining green areas low likelihood. Large channel networks tend to form mainly in low-likelihood areas. However, most of these channel networks terminate in medium or high-likelihood areas, corresponding to potential moulin locations.

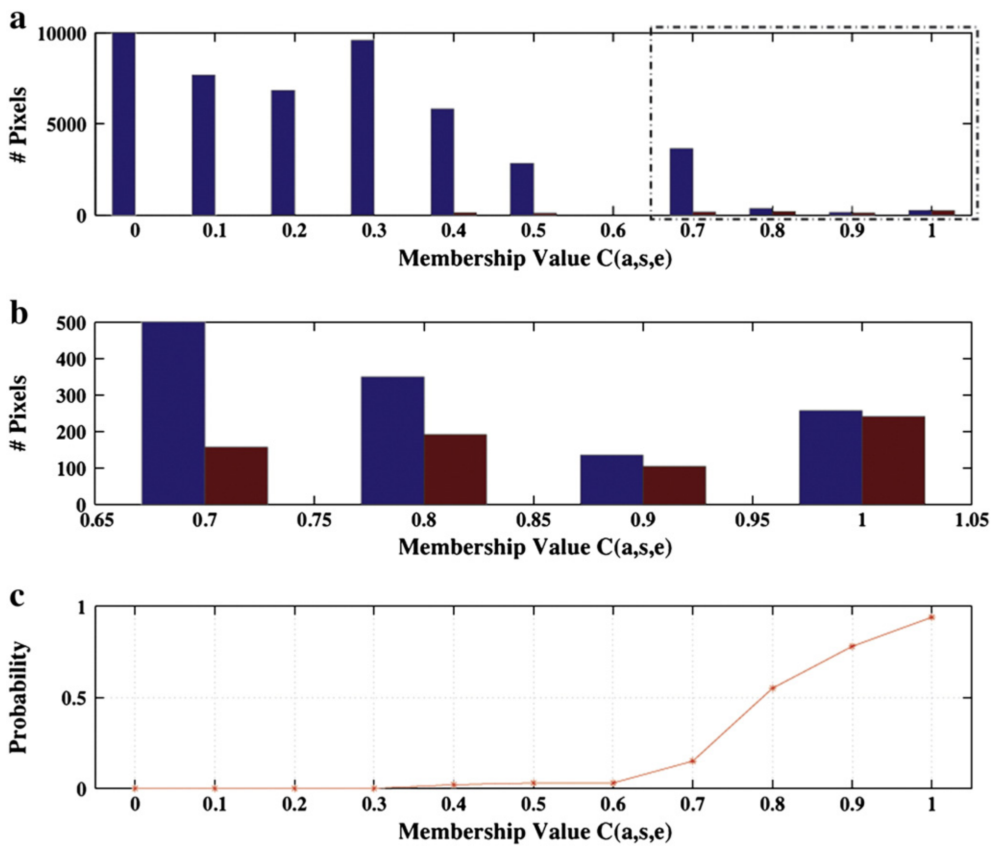

Fig. 4. (a) The histogram for the number of pixels for each membership ($C(a, s, e)$) value in the ablation zone. Blue bars correspond to all pixels and red bars indicate moulin-containing pixels. (b) Blow up of the dashed rectangle in (a) to accentuate the portion of interest with significant moulin occurrence. (c) Probability of moulin occurrence (# moulin containing pixels divided by total # pixels) as a function of $C(a, s, e)$. Although not shown, several pixels with $C(a, s, e) > 0.7$ contain more than one moulin. Specifically, clusters of up to 5 moulins per pixel were encountered with $C(a, s, e) \sim 0.8$.

6. Discussion

The fuzzy logic approach described here represents an encouraging first attempt to model the likelihood of moulin occurrence and the spatial distribution of moulins in the Western Greenland ablation zone. The three independent variables employed in this study are commonly used for simple parameterizations in topographic spatial analysis. This first-order modeling attempt aims to further the understanding of where moulins occur, and hence the locations where water can potentially reach the glacier bed and cause lubrication. Quantifying this process is important for constraining physically based ice sheet models. However, the topographic variables chosen here do not

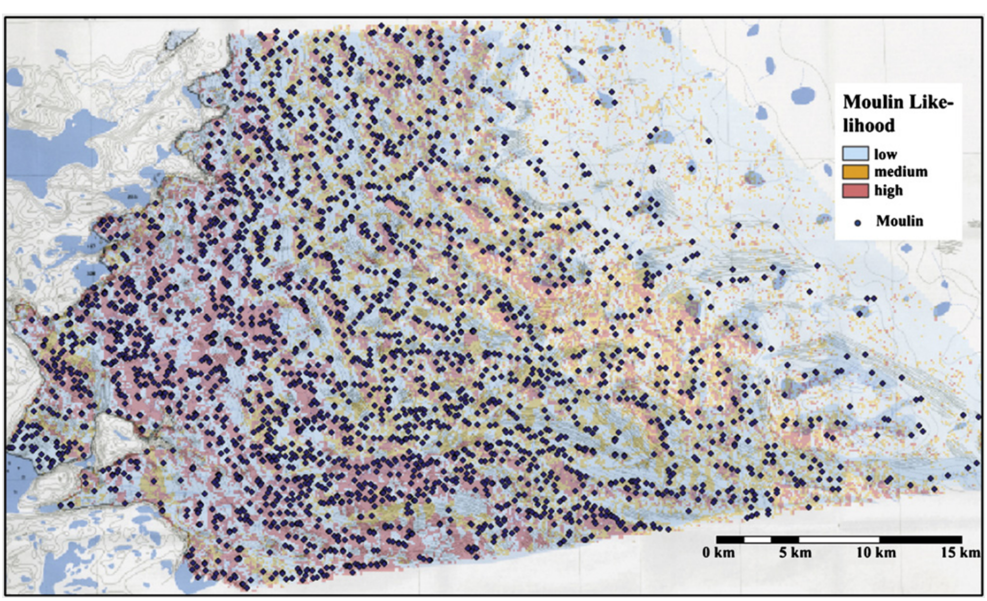

Fig. 5. The modeled moulin likelihood classes (high, medium, low) for 2008–09 overlain by the extracted moulin locations.

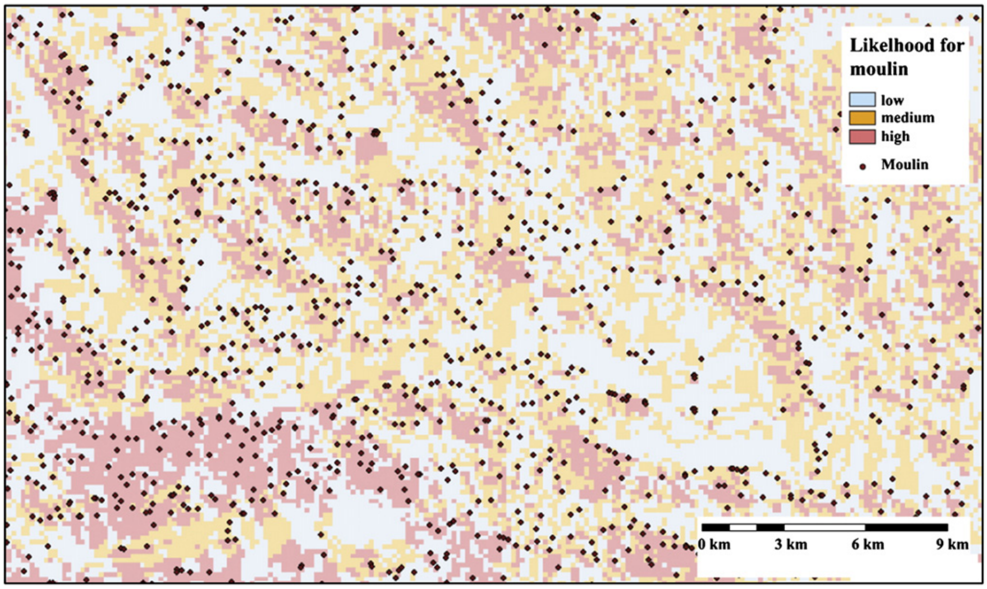

Fig. 6. Blow up of the southern most regions showing the moulin likelihood and the moulin locations for 2008. Note that the extracted moulins seem to form at the upslope edges of medium and high likelihood areas. The black arrows indicate the main flow direction.

explicitly represent the physical processes involved in moulin development. The present model does not rely on any basal topography or process-based modeling to calculate extensional strain rates that would enable the identification of crevassed areas that precondition ice for moulin formation downstream of crevasse fields.

Our results suggest that the fuzzy overlay operation and its 1985 membership function $C(a, s, e)$ remain valid for the quantification of moulin likelihood at later points in time, such as in 2008–09 when different data sources are used (e.g., ASTER DEM rather than GEUS DEM). The 2008–09 model easily accommodates increases in surface meltwater generation by using a critical meltwater volume necessary for moulins to develop calculated from the 1985 data.

Despite the difficulty of quantifying the accuracy of the model, we have been able to demonstrate the robustness of fuzzy membership functions for all variables (Fig. 2). Using subsets of the moulins in a Monte Carlo simulation we have been able to demonstrate that the distribution of moulins is not purely due to chance but is, at least, partially determined by the independent first-order local topographic variables. While we have validated this approach for the Sermeq Avannarleq region, a more extended validation of this methodology in different regions of the Greenland Ice Sheet runoff zone is warranted. This study focused on a first-order approach that has been able to demonstrate that moulins do not occur at random from a statistical point of view and those simple topographic variables and fuzzy sets allow locating areas of particularly high likelihood of moulin occurrence.

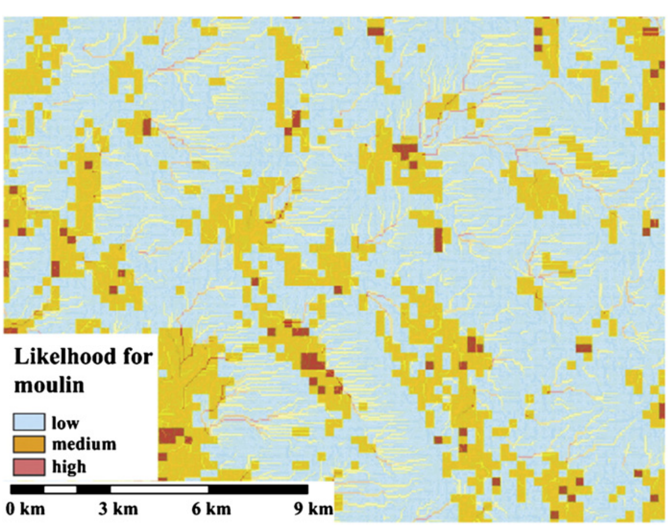

Fig. 7. Flow channels of the surface melt water run-off network (blue) run through or form in areas of low moulin likelihood. Many of these channels however terminate in the medium (orange) and high likelihood regions (red).

An absolute accuracy assessment of the model cannot be performed, as the total number of moulins and their absolute identification accuracy are unknown in both 1985 and 2008–09. The discrepancy in the total number of modeled moulin locations between 1985 and 2008–09 may indicate that only a subset of moulins was mapped in 1985. This could represent a possible reason for a model bias and result in different optimal membership functions. However, the presented approach was successful in predicting areas of high and medium moulin likelihood, and hence the locations where the water most likely penetrates the ice. Such an approach can help to quantify associations between changes in the topography of the runoff zone in Western Greenland (surface elevation, aspect and slope) in response to projected climate warming and moulin discharge to the glacier bed. Although our overall approach successfully identifies nearly 90% of the moulin locations, there is room for improvement. Fig. 5 and the close up Fig. 6 illustrate the high frequency of moulins along the upslope edges of the medium and high-likelihood areas. This indicates a strong influence of ice flow direction on the locations where moulins develop, which is not accounted for in our model. Future research will seek to enhance the presented approach by incorporating such higher-order topographic information. It is also important to develop numerically complex approaches for incorporating information/proxies on physical processes controlling moulin initiation. For instance, crevasse propagation and moulin occurrence are also influenced by ice stress and strain history, which can only be included into a moulin location model via a lagrangian scheme to trace the downstream advection of preconditioned ice.

7. Conclusions

We developed a model based on fuzzy set theory to predict moulin locations on the Sermeq Avannarleq in Western Greenland using three common topographic independent variables. The model was able to correctly identify 92% of the moulin locations in a 1985 training dataset. In two sub-regions where precise data on moulin locations was available for 2008–09, the model correctly predicted slightly fewer than 90% of the moulins. We also showed that rather than using crisp alpha cuts to delineate moulin occurrence probability, it is more appropriate to use a range of alpha cuts.

Acknowledgments

This research was supported by NASA Cryosphere Science Program grants NNX08AT85G and NNX07AF15G and the NSF DDRI grant 0926911. WC thanks NSERC and CIRES for fellowship support. We would also like to thank two anonymous reviewers for their very valuable insights.

References

Alley, R. B., Dupont, T. K., & Parizek, P. R. (2005). Access of surface meltwater to beds of sub-freezing glaciers: Preliminary insights. *Annals of Glaciology*, *40*, 8–14.

Anderson-Tarver, C., Leyk, S., & Buttenfield, B. P. (2011). *Fuzzy modeling of geometric textures for area-patch generalization.* Cartography and geographical information science.

Arnot, C., Fisher, P. F., Wadsworth, R., & Wellens, J. (2004). Landscape metrics with ecotones: Pattern under uncertainty. *Landscape Ecology*, *19*, 181–195.

Bolliger, J., & Mladenoff, D. J. (2005). Quantifying spatial classification uncertainties of the historical Wisconsin landscape (USA). *Ecography*, *28*(2), 141–156.

Burrough (1989). Fuzzy mathematical methods for soil survey and land evaluation. *Journal of Soil Science*, *40*, 477–492.

Catania, G., & Neumann, T. (2010). Persistent englacial drainage features in Greenland Ice Sheet. *Geophysical Research Letters*, *37*, L02501. doi:10.1029/2009GL041108.

Colgan, W., Rajaram, H., Anderson, R., Steffen, K., Phillips, T., Joughin, I., Zwally, H., Abdalati, W. (2011). The annual glaciohydrology cycle in the ablation zone of the Greenland Ice Sheet: Part 1. Hydrology Model. J. Glaciol. 10J154.

Corne, S., Murray, T., Openshaw, S., See, L., & Turton, I. (1999). Using computational intelligence techniques to model subglacial water systems. *Journal of Geographical Systems*, *1*, 37–60.

Cuffey, K. M., & Clow, G. D. (1997). Temperature, accumulation, and ice sheet elevation in central Greenland through the last deglacial transition. *Journal of Geophysical Research*, *102*(C12), 26,383–26,396.

Das, S. B., Joughin, I., Behn, M. D., Howat, I. M., King, M. A., Lizarralde, D., et al. (2008). Fracture propagation to the base of the Greenland ice sheet during supra-glacial lake drainage. *Science*, *320*, 778–781.

Deng, Y., & Wilson, J. P. (2008). Multi-scale and multi-criteria mapping of mountain peaks as fuzzy entities. *International Journal of Geographical Information Science*, *22* (2), 205–218.

Dubois, D., & Prade, H. (1988). Fuzzy sets and systems. New York: Academic Press.

Fausto, R. S., Ahlstrøm, A. P., van As, D., & Bøggild, C. E. (2009). A new present-day temperature parameterization for Greenland. *Journal of Glaciology*, *55*(189), 95–105.

Fisher, P. (2000). Sorites paradox and vague geographies. *Fuzzy Sets and Systems*, *113*, 7–18.

Fisher, P., Wood, J., & Cheng, Tao (2004). Where is Helvellyn? Fuzziness of multi-scale landscape morphometry. *Transactions of the Institute of British Geographers*, *29*(1), 106–128.

Fountain, A. G., Schlichting, R. B., Jansson, P., & Jacobel, R. W. (2005). Observation of en-glacial water passages: A fracture dominated system. *Annals of Glaciology*, *40*, 25–29.

Fountain, A. G., & Walder, J. S. (1998). Water flow through temperate glaciers. *Reviews of Geophysics*, *36*(3), 299–328.

Fritz, S., & See, L. (2005). Comparison of land cover maps using fuzzy agreement. *International Journal of Geographical Information Science*, *19*(7), 787–807.

Greuell, W. (2000). Melt-water accumulation on the surface of the Greenland ice sheet: Effect on albedo and mass balance. *Geografiska Annaler*, *82A*, 488–497.

Gulley, J., & Benn, D. (2007). Structural control of en-glacial drainage systems in Himalayan debris-covered glaciers. *Journal of Glaciology*, *53*(181), 399–412.

Hanna, E., Huybrechts, P., Steffen, K., Cappelen, J., Huff, R., Shuman, Ch., et al. (2008). Increased runoff from melt from the Greenland ice sheet: A response to global warming. *Journal of Climate*, *21*, 331–341.

Holmlund, P. (1988). Internal geometry and evolution of moulins, Storglaciaren, Sweden. *Journal of Glaciology*, *34*(117), 242–248.

Hooke, R. L. (2005). Principles of glacier mechanics Cambridge University Press.

Howat, I. M., Joughin, I., Fahnestock, M., Smith, B. E., & Scambos, T. A. (2008). Synchronous retreat and acceleration of southeast Greenland outlet glaciers 2000–06: Ice dynamics and coupling to climate. *Journal of Glaciology*, *54*(187), 646–660.

Joughin, I., Das, S. B., King, M. A., Smith, B. E., Howat, I. M., & Moon, T. (2008). Seasonal speedup along the western flank of the Greenland ice sheet. *Science*, *320*, 781–783.

Key, J. R., Maslanik, J. A., & Barry, R. G. (1989). Cloud classification from satellite data using a fuzzy sets algorithm: A polar example. *International Journal of Remote Sensing*, *10*(12), 1823–1842.

Klir, G. J., & Yuan, B. (1995). Fuzzy sets and fuzzy logic: Theory and applications. Upper Saddle River, NJ: Prentice-Hall.

Leyk, S., & Zimmermann, N. E. (2007). Improving land change detection based on uncertain survey maps using fuzzy sets. *Landscape Ecology*, *22*, 257–272.

McBratney, A. B., & Odeh, I. O. A. (1997). Application of fuzzy sets in soil science: Fuzzy logic, fuzzy measurements and fuzzy decisions. *Geoderma*, *77*, 85–113.

Montgomery, & Runger (2006). Applied statistics and probability for engineers Wiley Publications.

Paterson, W. S. B., & Cuffey, K. (2010). The physics of glaciers Pergamon Press.

Phillips, T. P., Rajaram, H., & Steffen, K. (2010). Cryo-hydrologic warming: A potential mechanism for rapid thermal response of ice sheets, GRL, 2010GL044397.

Piccini, L., Romeo, A., & Badino, G. (2002). Moulins and marginal contact caves in the Gornergletscher, Switzerland. *Nimbus*, *23–24*, 94–99.

Reynaud, L. (1987). The November 1986 survey of the grand moulin on the Mer de Glace, Mont Blanc massif, France. *Journal of Glaciology*, *33*(117), 130–131.

Rignot, E., Bamber, J., van den Broeke, M., Davis, C., Li, Y., van de Berg, W., et al. (2008a). Recent mass loss of the Antarctic Ice Sheet from dynamic thinning. *Nature Geosciences*. doi:10.1038/ngeo102.

Rignot, E., Box, J. E., Burgess, E., & Hanna, E. (2008b). Mass balance of the Greenland ice sheet from 1958 to 2007. *Geophysical Research Letters (GRL)*. doi:10.1029/2008GL035417.

Rignot, E., & Kanagaratnam, P. (2006). Changes in the velocity structure of the Greenland ice sheet. *Science*, *311*, 986–990.

Robinson, V.B. (2003). A Perspective on the fundamentals of fuzzy sets and their use in geographic information systems, 7(1), 3–30.

Robinsson, V. B. (1988). Some implications of fuzzy set theory applied to geographic databases. *Computers, Environment and Urban Systems*, *12*(2), 85–97. doi:10.1016/0198-9715(88)90012-9.

Tarboton, D. G., Bras, R. L., & Rodriguez–Iturbe, I. (1991). On the Extraction of channel networks from digital elevation data. *Hydrological Processes*, *5*, 81–100.

Thomsen, H. H. (1986). Photogrammetric and satellite mapping of the margin of the inland ice, West Greenland. *Annals of Glaciology*, *8*, 164–167.

Thomsen, H. H., Thorning, L., & Braithwaite, R. J. (1988). *Glacier-hydrological conditions on the inland ice northeast of Jakobshavn/Ilulissat, West Greenland.* Rapport 138, Groenlands Geologiske Undersoegelse.

Van den Broeke, M., Bamber, J., Ettema, J., Rignot, E., Schrama, E., van de Berg, W. J., et al. (2009). Partitioning recent Greenland mass loss. *Science*, *326*(5955), 984–986. doi:10.1126/science.1178176.

Van der Veen, C. J. (2007). Fracture propagation as means of rapidly transferring surface meltwater to the base of glaciers. *Geophysical Research Letters*, *34*, L01501. doi:10.1029/2006GL028385.

Velicogna, I., & Wahr, J. (2006). Measurements of time-variable gravity show mass loss in Antarctica. *Science*, *311*(5768), 1754–1756. doi:10.1126/science.1123785.

Yager, R. R. (1980). On a general class of fuzzy connectives. *Fussy Sets and Systems*, *4*, 235–242.

Yager, R. R. (1995). Aggregation operators and fuzzy systems modeling. *Fuzzy Sets and Systems*, *67*, 129–146.

Zadeh, L. A. (1965). Fuzzy sets. *Information and Control*, *8*(3), 338–353.

Zwally, H. J., Abdalati, W., Herring, T., Larson, K., Saba, J., & Steffen, K. (2002). Surface melt induced acceleration of Greenland ice-sheet flow. *Science*, *297*, 218–222.